Bulletin of the Seismological Society of America. Vol. 65, No. 5, pp. 1407–1418. October 1975.

A SEARCH FOR TRAVEL-TIME CHANGES ASSOCIATED WITH THE PARKFIELD, CALIFORNIA, EARTHQUAKE OF 1966

By David M. Boore, Allan G. Lindh, Thomas V. McEvilly, and Wayne W. Tolmachoff

Abstract

Studies of P-wave travel times at a station within 0.5 km of the ground rupture associated with the Parkfield, California, earthquake of 1966 show no systematic variations for a time period of 7 months before the mainshock to at least 13 months after the event. Sources used include quarry blasts, regional earthquakes, explosions at the Nevada Test Site (NTS), and teleseismic earthquakes. The data from the quarry blasts and regional earthquakes have a scatter of less than ± 0.15 sec. With suitable source corrections, the scatter in the NTS data can be reduced to about ± 0.25 sec (making the catalog of nuclear explosions potentially useful for monitoring large travel-time changes). The data from teleseismic P waves have much more scatter than do the data from the more local sources.

The regional earthquake data (expressed as the time differences between the station near the ground rupture and one farther to the north) show temporal variations, but these variations appear to be due to systematic changes in the hypocentral locations of the sources rather than changes in the seismic velocity near the recording stations. The quarry blasts are not as subject to this bias and consequently are more reliable for the monitoring of seismic velocity changes.

The negative results of our study do not rule out the possibility that a velocity anomaly was associated with the Parkfield earthquake; they do, however, require that any velocity change as large as 15 per cent be confined to a volume that is either less than about 5 km deep by several kilometers wide or that does not coincide spatially with the rupture zone.

Introduction

We have looked for seismic velocity changes associated with the 1966 Parkfield earthquake by studying P-wave travel times from a number of sources before and after the event. The main shock ($M_L = 5.5$, $m_b = 5.8$, $M_S = 6.4$), was preceded by a number of small to moderate events. An extensive series of aftershocks followed the main shock (see McEvilly *et al.*, 1967 and Eaton *et al.*, 1970, for a summary of the activity). Fortunately, a high-quality seismic station (GHC) was operating prior to the Parkfield sequence in what was to be the midst of the aftershock area (Figure 1). Unfortunately, the station was in existence for only about 8 months before the earthquake. In spite of this shortcoming, the data provided a unique opportunity to investigate a larger earthquake on the San Andreas fault than has been available in previous studies.

Data

An important feature of our study is the availability of well-located energy sources outside the region of the earthquake. The following sources of P waves were used (Figure 1) with distances to GHC in parentheses: explosions at the Natividad (149 km) and Basalt Hill (148 km) quarries, small earthquakes ($M_L \approx 2.5$) in the Bear Valley and Stone

Canyon region of the San Andreas fault (107 to 124 km), nuclear explosions at the Nevada Test Site (about 400 km), and earthquakes at teleseismic distances (> 16°).

The primary recording stations were Priest (PRI) and Gold Hill (GHC). PRI and GHC are more or less in line with all the sources except those at the Nevada Test Site (NTS) and the teleseisms. Readings from Llanada (LLA) and Jamestown (JAS) were used to

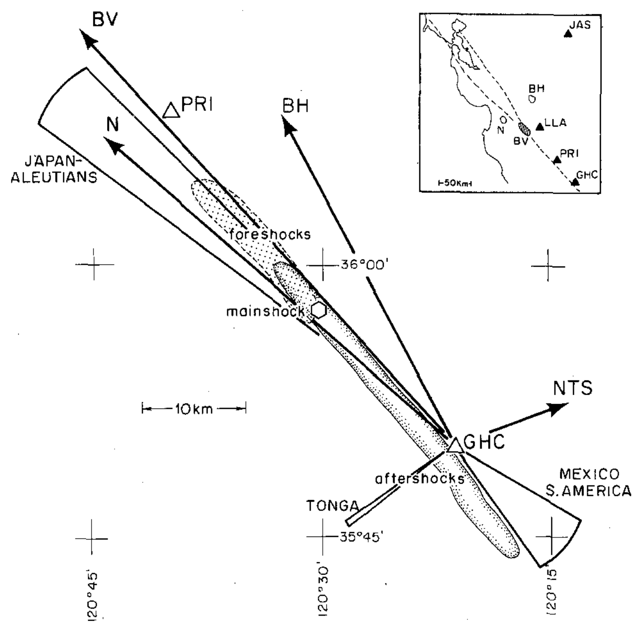

FIG. 1. Location map showing GHC and PRI, directions to sources, and zones of foreshock and aftershock activity of the Parkfield earthquake (using locations from McEvilly *et al.*, 1967, and Eaton *et al.*, 1970). *Inset*: regional map showing station and quarry locations. The dashed line indicates the San Andreas fault, with the Bear Valley-Stone Canyon region shown by the shaded area.

provide a check on the stability of residuals at PRI. PRI, LLA and JAS are operated by the Seismographic Station of the University of California at Berkeley. The output of these stations is telemetered to Berkeley where it is recorded on 16-mm film. McEvilly and Johnson (1974) describe the system characteristics and timing procedures (timing accuracy is better than 0.1 sec). GHC was a three component, short-period station installed during October, 1965. The data were recorded on 35-mm film at the site. Each component plus

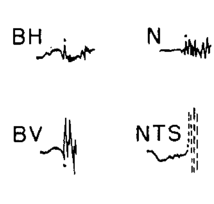

FIG. 2. Examples of vertical component records at GHC showing phases picked.

a radio time trace was recorded on individual films, with internal chronometer marks supplying a link between the different films (see Eaton, 1967, for a more complete description). The events were timed to 0.05 sec on permanent enlargements of the 35-mm film. We estimate the timing accuracy to be ± 0.1 sec or better for local events and ± 0.2 sec for the teleseisms.

The initial P arrival was timed for the teleseisms. The P_n phase was picked for the NTS events; this was the first arrival on the record (Figure 2 shows a typical record). Arbitrary but unique phases (peaks or troughs) in the first cycles of motion were picked on the recordings of the other events (Figure 2). These phases are associated with some type of crustal reflection or refraction. Transparent overlays were used as much as possible for

TABLE 1

BASALT HILL*

Date (month day)	LLA (hr:min:sec)	PRI-LLA (sec)	GHC-PRI (sec)
1965			
12–20	23 : 39 : 54.05	10.60	7.60
12–27	23 : 45 : 32.25	10.70	7.55
1966			
1–25	23 : 41 : 30.15	10.65	7.60
1–27	23 : 38 : 28.65	10.65	—
3–03	23 : 41 : 03.15	10.65	7.55
3–16	23 : 32 : 53.8	10.65	7.50
3–24	23 : 43 : 39.9	10.65	7.60
4–06	23 : 38 : 02.9	10.60	—
4–21	23 : 32 : 37.5	10.60	7.55
4–28	22 : 47 : 59.2	10.70	7.55
5–05	22 : 50 : 32.9	10.70	7.55
6–02	22 : 49 : 14.6	10.60	7.60
6–15	22 : 41 : 28.95	10.70	7.55
7–26	22 : 35 : 09.8	10.65	7.65
8–04	18 : 30 : 22.35	10.70	7.50
8–09	22 : 39 : 03.7	10.70	7.60
8–15	22 : 37 : 07.45	10.65	7.62
8–19	22 : 42 : 21.15	10.70	7.52
9–08	17 : 59 : 31.7	10.70	—
9–14	22 : 38 : 36.35	10.65	7.50
9–23	22 : 32 : 58.75	10.60	—
10–10	22 : 44 : 29.0	10.65	7.60
10–25	22 : 34 : 33.2	10.75	—
12–01	23 : 08 : 01.75	10.65	7.60
12–22	23 : 36 : 27.2	10.60	—
1967			
1–05	19 : 33 : 16.7	10.60	—
1–18	23 : 43 : 03.8	10.65	7.55
2–09	23 : 35 : 50.7	10.65	—
2–23	23 : 38 : 00.7	10.70	—
3–08	23 : 32 : 29.0	10.65	—
3–22	23 : 38 : 51.0	10.70	7.55

* Data used in Figure 3.

positive identification of the phases. With a few exceptions, the Z (vertical) component was used for all the readings at GHC.

The reduced data for the local sources are shown in Figure 3 and are listed in Tables 1, 2 and 3. The time differences PRI–LLA and GHC–PRI for the Basalt Hill (BH) data (104 km from PRI) are shown in the top two bands of Figure 3. The Natividad (N) data (105 km from PRI) in the third band are referred to the inferred origin time of the blasts

(McEvilly and Johnson, 1974). The time difference between GHC and PRI is used for the Bear Valley (BV) earthquakes (fourth band).

The best data, in terms of stability of wave forms and frequency of occurrence, are the quarry blasts at Basalt Hill. The GHC-PRI times for these blasts, as well as a running mean over 5 points, have been plotted at an expanded scale in Figure 4. The scatter in the means is ± 0.02 sec. There are not enough Natividad quarry blasts to calculate a running mean, but the scatter of the points shown in Figure 3 (± 0.10 sec) is similar to the total scatter in the BH data (± 0.08 sec). Thus, any time variations contained in the quarry blast data must be considerably less than about ± 0.10 sec.

TABLE 2

NATIVIDAD*

Date (month day)	Origin Time (hr:min:sec)	GHC-O (sec)
1965		
11–09	22:58:55.10	24.57†
1966		
5–27	23:21:26.30	24.50†
6–15	22:28:53.80	24.4
6–29	21:57:56.05	24.6
11–02	23:24:32.70	24.6
1967		
1–19	23:00:58.50	24.45
8–03	22:32:11.15	24.55

* Data used in Figure 3.

† T component corrected to Z using readings from June 15, 1966 and November 2, 1966.

TABLE 3

REGIONAL EARTHQUAKES*

Date (month day)	Origin Time (hr:min)	Epicenter Distance (km)	Depth (km)	GHC-PRI (sec)
1966				
1–03	23:49	107	10	6.95
3–09	04:11	113	5	6.87
5–04	06:32	115	8	6.75
8–05	05:54	116	6	6.70
10–20	08:00	124	7	6.75
10–20	14:58	124	4	6.75
10–20	15:10	124	5	6.65
1967				
1–17	11:13	120	6	6.85
5–25	05:21	109	4	7.05
7–24	05:37	111	9	6.95
8–03	05:33	109	8	6.95

* Data used in Figure 3.

In contrast to the quarry blast data are the results from the regional earthquakes near Bear Valley (BV), which show a scatter of ± 0.20 sec. This scatter is associated with a consistent trend in the data (Figure 3). From Figure 1, we see that the path from BV passes closer to the aftershock zone than does the path from BH; thus the BV data may be more sensitive than the BH data to any velocity variations associated with the earthquake. Note, however, that the path from Natividad is similar to the path from BV, and yet the scatter in the Natividad data is only half as great. We suspect that the trends seen in the BV data

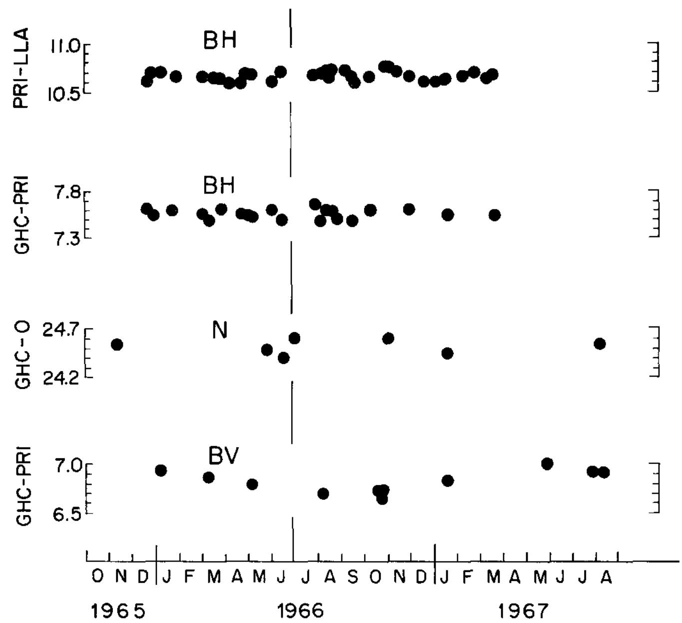

FIG. 3. Data for the regional events to the northwest, plotted against time of occurrence. The ordinates are in seconds. The date of the mainshock is given by the vertical line. The reading error is somewhat less than twice the width of a dot.

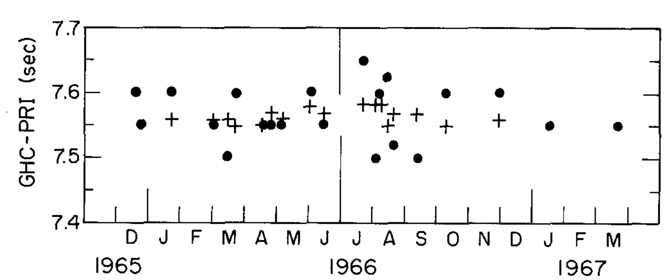

FIG. 4. GHC-PRI residuals for BH events plotted at an expanded scale. Crosses are from a running mean over 5 points. The mainshock time is given by the vertical line.

are not due to velocity changes, but are due to systematic changes in the locations of the BV events. The BV events define two groups: those which are spread out along the fault (A in Figure 5) and those which form a cluster at the southeastern end of the set of events (B in Figure 5). In contrast to the A events, the wave forms of the B events showed considerable variation and were difficult to correlate with one another. The data included in Table 3 represent our best attempt at correlating the wave forms. As shown by the symbols in Figure 5, only five of the 10 events in group B which did not saturate the

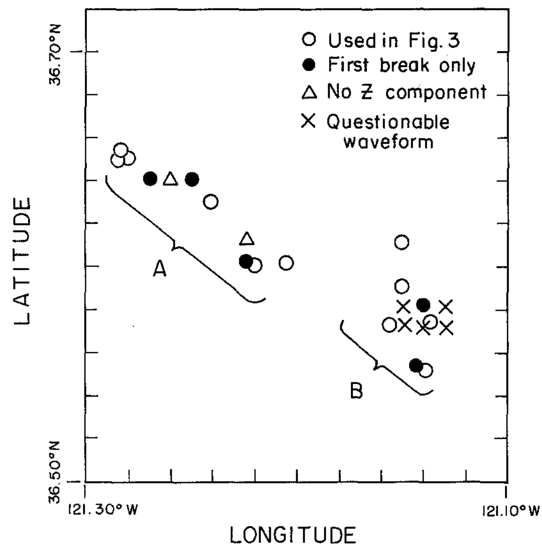

FIG. 5. Epicenters of regional earthquakes, showing grouping into sets A and B. The symbol used for plotting indicates the status of the GHC recording. Note the number of events in group B whose wave forms could not be correlated with the other events in sets A and B. The first breaks were not used because they could not be timed as accurately as the characteristic second phase.

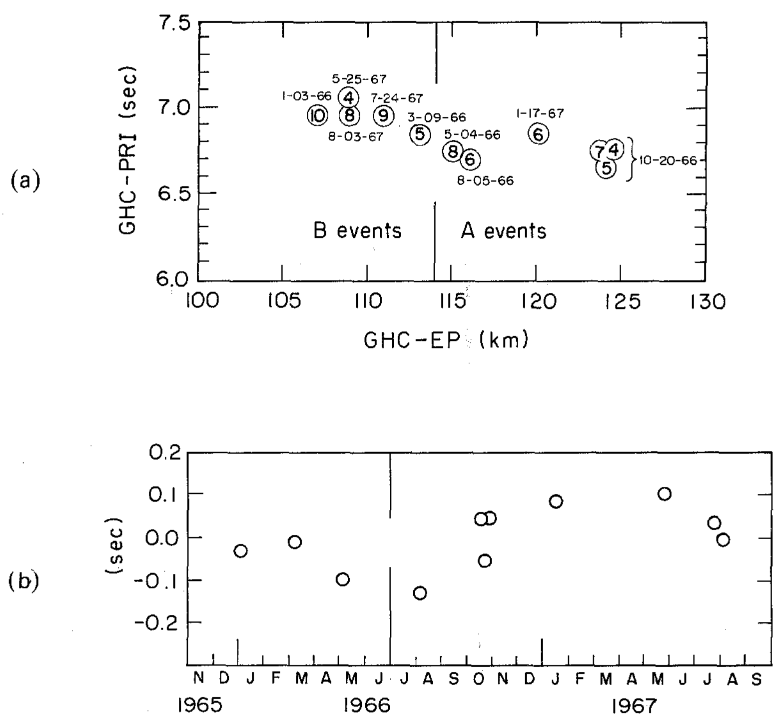

FIG. 6. (a) Bear Valley data (GHC-PRI) plotted against epicentral distance. The date and depth (in kilometers) are given for each point. Note that the ordinate is drawn to a different scale than in Figure 3. The vertical line separates group B and group A events. (b) The residuals plotted against time after removing a linear regresssion line from the data in (a). The vertical line shows the time of the main event.

instrument on the first arrival were correlatable. When GHC-PRI residuals are plotted against epicentral distance (Figure 6a), the residuals from the B events are late relative to those from the A events. A systematic decrease in GHC-PRI time of 0.2 to 0.3 sec with increasing epicentral distance is suggested, with a possible decrease of 0.1 to 0.2 sec with increasing focal depth at a given distance. Such systematic changes might be expected for travel times in a crust in which velocity increases with depth. Fitting a straight line to the data in Figure 6a and plotting the residuals (Figure 6b) from this line as a function of time reduces the scatter (from ± 0.20 to ± 0.12 sec), but produces a new trend in the data (increasing residuals with increasing time). The correlation with epicentral distance may

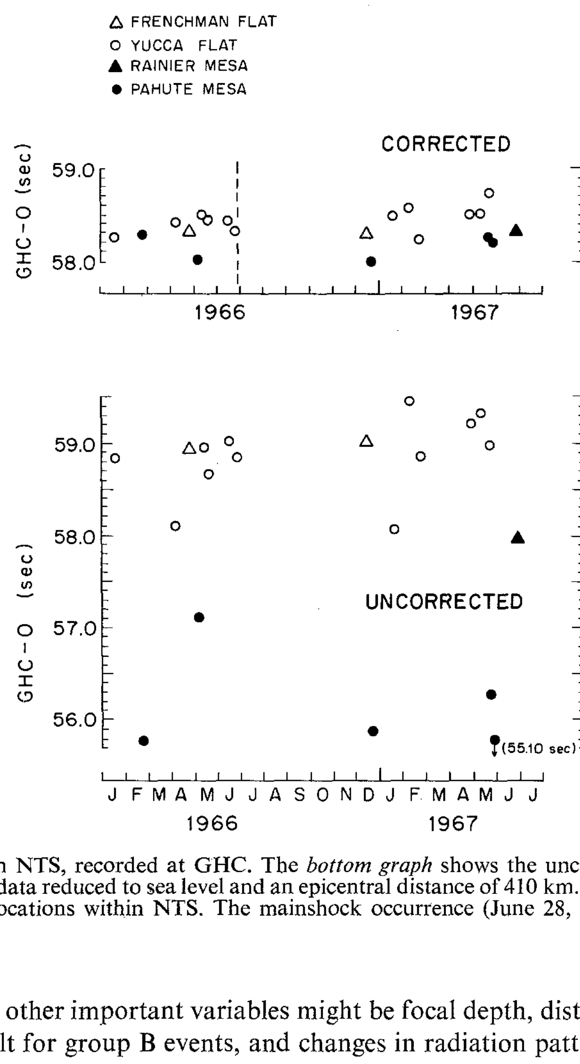

FIG. 7. Data from NTS, recorded at GHC. The *bottom graph* shows the uncorrected data, and the *top* shows the same data reduced to sea level and an epicentral distance of 410 km. The symbols represent blasts at different locations within NTS. The mainshock occurrence (June 28, 1966) is shown by the dashed line.

not be sufficient; other important variables might be focal depth, distance away from the San Andreas fault for group B events, and changes in radiation pattern. Unfortunately, there are not enough data to make correlations among all of these parameters. Although we cannot absolutely rule out the existence of time variations related to changes in seismic velocity, there are clear source biases in the BV data shown in Figure 3. The source effects can explain almost all of the variation in the data. Any residual due to velocity changes is probably less than about ± 0.06 sec.

The conclusion follows from Figures 3, 4, and 6 that no anomalous changes have been observed, within the accuracy of our data, for a period of at least 7 months before and 13 months after the main shock. This can be compared with the results of Robinson *et al.* (1974), who found evidence for a velocity change to the north along the San Andreas fault; the scatter in their data is ± 0.10 to ± 0.15 sec, and the anomaly corresponds to an offset of about 0.25 sec in the mean of the data points. Such an anomaly would be very obvious in our data.

The NTS data, presented in Figure 7, represent absolute travel times from an equivalent sea level source to GHC (reduced to sea level by adding a correction of -0.09 sec), with the source-receiver distance normalized to 410 km. The correction procedure is discussed in the Appendix. The lower band shows the data uncorrected for local site

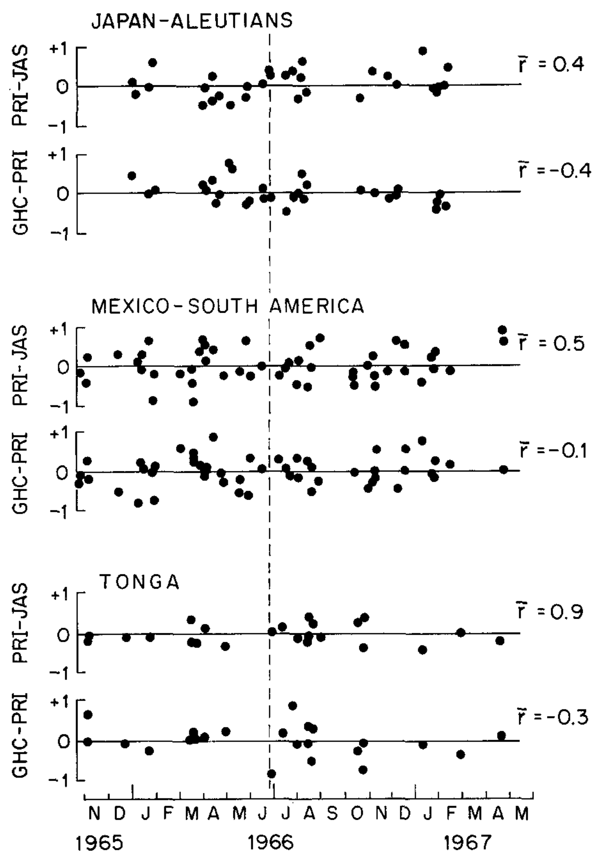

FIG. 8. Data from teleseisms. Plotted are the two-station differences in the residuals from the Herrin (1968) tables. Data from three separate azimuths are shown. The mean of the data (shown on the right side, in seconds) was removed before plotting. The ordinates are in seconds; note that the scale is different from that used in Figure 3. The mainshock occurrence is given by the vertical dashed line.

geology or distance away from the 410-km norm. The upper band shows the corrected data. The scatter has been reduced somewhat. The Pahute Mesa data contain a bias of approximately 0.3 sec, presumably due to an inadequacy in the correction procedure. Allowing for this bias, the data before the main shock are nearly as accurate (± 0.15 sec) as those of Robinson *et al.* (1974), but an anomaly comparable to theirs is clearly not present. The data after the main shock show more scatter (± 0.25 sec) than before. The small amount of scatter in the quarry blast and regional earthquake data in the 4 months following the main shock, however, leads us to attribute the increased scatter in the NTS data to variations in geology throughout the source area.

In view of the excellence of the quarry blast and earthquake data, the main reason for including the data in Figure 7 is to show the accuracy that can be expected from NTS data. Many explosions with accurate timing and locations have been detonated at NTS (Springer and Kinnaman, 1971), and the data set may have some value for monitoring temporal changes in velocity (e.g., Utsu, 1974). With the considerable scatter, however, travel-time changes approaching 0.4 sec would be needed.

Data from teleseisms are shown in Figure 8 for events at various azimuths. The two-station delay times were found by differencing the station residuals formed from the observed and computed travel times, using the Herrin (1968) tables as a reference. The readings at PRI and JAS were obtained from volumes 35 and 36 of the University of California's *Bulletin of the Seismographic Stations* and the GHC readings were measured from enlargements of the 35-mm film strips. The scatter in the data was reduced considerably by using two-station differences. The data have been culled by eliminating all residuals outside of ± 1 sec from the overall mean. Travel-time variations of 0.25 sec or more could be masked by the scatter in the data (Figure 8), although indications of trends can be seen on some of the plots. A comparison of these data with those from the quarry blasts and regional earthquakes (Figure 3) argues against the reality of any of the trends, and points up the difficulty in using teleseisms for precise estimation of velocity changes. The scatter in Figure 8 could undoubtedly be reduced by rereading the data (e.g., compare with the results of Cramer and Kovach, 1974), but this did not seem worthwhile considering the quality of the other data available to us. The scatter emphasizes the caution necessary in using published data. Wyss (1974) also studied teleseismic residuals at PRI and JAS, using a much larger data base. He found a change of about 0.4 sec at PRI, during 1966, but this largely disappeared when he subtracted residuals from several stations.

Discussion

A number of studies have looked for premonitory changes in seismic velocities along the central San Andreas fault. Robinson *et al.* (1974) found evidence for *P*-wave delays prior to a magnitude 5.1 earthquake on February 24, 1972. Other studies, however, have not seen any changes (Cramer and Kovach, 1974; McEvilly and Johnson, 1973 and 1974; Bakun *et al.*, 1973). These other studies are not inconsistent with the observations of Robinson *et al.* (1974), who point out (personal communication, 1974) that the small size of the anomalous zone and the masking effects of diffraction around the zone require a fortuitous combination of sources and receivers, which is not usually available.

In our study, GHC was in an almost ideal location (Figure 1) and the absence of an anomaly puts some constraints on the location and size of any zone of time-varying velocity. First, it is possible that no velocity anomaly was associated with the earthquake, although the positive results for a significantly smaller earthquake 100 km or so to the northwest argues for some premonitory velocity change. It should be noted, though, that the 5.1 Bear Valley earthquake may have had a much larger stress drop than the Parkfield event (Aki, 1968; Johnson and McEvilly, 1974) and many other San Andreas earthquakes (Thatcher and Hanks, 1973). As yet insufficient data exist to delineate what relations, if any, exist between stress drops and velocity anomalies, but intuition suggests that higher stress drops imply larger shear stresses, at least in the focal region, and might accompany larger dilatant volumes.

Another possibility is that the anomaly had returned to normal before the installation of GHC (8 months before the main shock). Based on the precursor time observed by Robinson *et al.* (1974) (2 months for a magnitude 5.1 earthquake) and the precursor-time versus magnitude information gathered by Scholz *et al.* (1973), the precursor time for the Parkfield earthquake would be in the range 140 to 500 days. Since the actual duration of anomalous travel time can be as little as one-half the total precursor time, there is a remote chance that the 230 days of pre-mainshock recording at GHC missed the anomaly.

If we assume, however, that a velocity anomaly was present in the vicinity of the Parkfield earthquake during the recording period at GHC, our data put constraints on either the size or the location of the anomaly. We can make a crude estimate of the maximum change in velocity consistent with our data. Figure 9 is a cross section along the fault, showing the zones of fore- and aftershock activity. A range of possible ray paths for the events to the NW are shown. If we assume that all of the velocity change takes place within the aftershock zone and that our threshold of detectability is 0.20 sec [this is a conservative estimate and applies to the regional earthquake data; we could probably detect much smaller changes along the travel path from the Basalt Hill quarry (see Figure 4)], then changes in velocity of less than 9 per cent may have gone unnoticed. This should be compared with the estimated 10 to 15 per cent change found farther north along the San Andreas fault by Robinson *et al.* (1974). On the other hand, if the anomalous zone were only half as large as shown in Figure 9 the time delay introduced by material having a velocity 10 to 15 per cent slower than the surrounding medium might

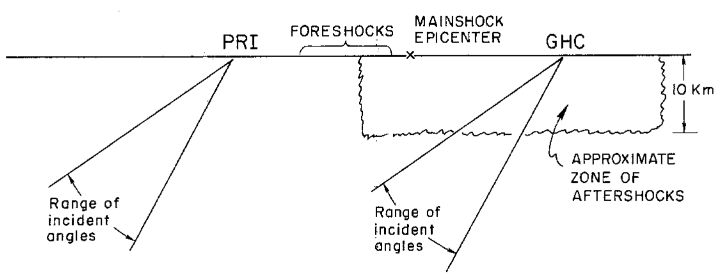

FIG. 9. A profile along the fault, showing possible ray paths for regional events to the northwest and the zones of fore- and aftershock activity.

not be noticed. (Scholz *et al.*, 1969, provide evidence that the vertical extent of the mainshock rupture was only half as large as the zone defined by aftershocks.) Furthermore, the smaller the zone of material with anomalous velocity, the greater the chance that diffraction will mask the zone. Thus, it might be possible for a zone 5 km in depth and several kilometers in width, with velocities 10 to 15 per cent slower than the surroundings, to exist undetected under GHC. We can, however, exclude with some confidence an anomalous zone several source dimensions in size as has been invoked to explain apparent velocity changes elsewhere (Whitcomb *et al.*, 1973; Aggarwal *et al.*, 1975).

It is also possible that an anomalous zone existed, but did not coincide in space with the rupture zone. As seen in Figure 1, the foreshock activity was northwest of the main epicenter. An anomalous zone there, or one confined to a small volume around the hypocenter, would not have been detected in our experiment (see Figure 9). A noncoincidence of the rupture zone and the anomalous zone might imply a highly nonuniform stress distribution prior to the earthquake, and would have important implications for the prediction of large earthquakes, regardless of the surveillance method.

In summary, *P*-wave residuals at GHC were stable for the 8 months prior to the Parkfield earthquake, despite a reasonable expectation, on the basis of work elsewhere, that an anomaly should have been seen. The simplest explanation, albeit a discouraging one, and the explanation with the greatest implications for both prediction attempts and source mechanism studies, is that not all moderate earthquakes are preceded by detectable velocity anomalies.

Acknowledgments

We thank the Office of Earthquake Research, U.S. Geological Survey for providing the GHC data and facilities for the enlargements of the films. Karen McNally of the University of California (Berkeley) kindly provided the relocated hypocenter parameters for the Bear Valley earthquakes. Discussions with Robert A. Page of the U.S. Geological Survey stimulated the research in this paper; John H. Healy of the USGS provided useful comments on the presentation.

Appendix

Correction of NTS Data

The complex geology in the NTS region leads to significant lateral variations in seismic velocity, and thus it is difficult to completely remove site-dependent variations in the travel times. Our simple procedure amounted to a stripping of the layers between sea level and the receiver and source stations followed by reduction to a common epicentral distance. The standard formula for the travel time of the critically refracted ray at the bottom of a stack of flat lying layers was used. In our case, the Mohorovičić discontinuity was the critical refractor, with a refractor velocity of 7.9 km/sec (Carder *et al.*, 1970).

For explosions on Pahute and Rainer mesas, the crustal velocity structure was taken from Table 1 of Hamilton and Healy (1969). The following P velocities were assumed for events in Yucca and Frenchman flats: 1.0 km/sec for the alluvium above the water table, 2.5 km/sec for the alluvium-tuff sequence below the water table, and 6.0 km/sec for the Paleozoic bedrock. These velocities are consistent with those given by Hazlewood *et al.* (1963) and Hamilton *et al.* (1970). The origin times, locations, surface elevation, shot depth, depth to water table, and depth to Paleozoics were taken from Springer and Kinnaman (1971).

References

Aki, K. (1968). Seismic displacements near a fault, *J. Geophys. Res.* **73** 5359–5376.

Aggarwal, Y. P., L. R. Sykes, D. W. Simpson, and P. G. Richards (1975). Spatial and temporal variations in t_s/t_p and in P-wave residuals at Blue Mountain Lake, New York: application to earthquake prediction, *J. Geophys. Res.* **80**, 718–732.

Bakun, W. H., R. M. Stewart, and D. Tocher (1973). Variations in V_p/V_s in Bear Valley in 1972, *Proc. Conf. Tectonic Probl. San Andreas Fault*, R. L. Kovach and A. Nur, Editors, Stanford Univ. Press, Stanford, Calif., 453–462.

Carder, D. S., A. Qamar, and T. V. McEvilly (1970). Trans-California seismic profile–Pahute Mesa to San Francisco Bay, *Bull. Seism. Soc. Am.* **60**, 1829–1846.

Cramer, C. H. and R. L. Kovach (1974). A search for teleseismic travel-time anomalies along the San Andreas fault zone, *Geophys. Res. Lett.* **1**, 90–92.

Eaton, J. P. (1967). Instrumental seismic studies, in *The Parkfield-Cholame, California, Earthquakes of June–August 1966—Surface Geologic Effects, Water Resources Aspects, and Preliminary Seismic Data, U.S. Geol. Surv. Profess. Paper 579.*

Eaton, J. P., M. E. O'Neill, and J. N. Murdock (1970). Aftershocks of the 1966 Parkfield-Cholame, California, earthquake: a detailed study, *Bull. Seism. Soc. Am.* **60**, 1151–1197.

Hamilton, R. M. and J. H. Healy (1969). Aftershocks of the BENHAM nuclear explosion, *Bull. Seism. Soc. Am.* **59**, 2271–2281.

Hamilton, R. M., P. P. Orkild, D. D. Dickey, and J. C. Hall (1970). Earthquakes, surface fracturing and strain associated with the Cruet, Pod, and Calabash underground nuclear explosions at Yucca Flat, Nevada Test Site, October 29, 1969, *U.S. Geol. Surv. Report 474–94, N.T.S. Report NTS-229.*

Hazlewood, R. M., D. L. Healey, and C. H. Miller (1963). U.S. Geological Survey Investigations of Yucca Flat, Nevada Test Site, Part B. Geophysical Investigations, *Technical Letter NTS-45, Part B.*, 53 pp.

Herrin, E. (Chairman) (1968). 1968 Seismological Tables for *P* phases, *Bull. Seism. Soc. Am.* **58,** 1193–1241.

Johnson, L. R. and T. V. McEvilly (1974). Near-field observations and source parameters of central California earthquakes, *Bull. Seism. Soc. Am.* **64,** 1855–1886.

McEvilly, T. V., W. H. Bakun, and K. B. Casaday (1967). The Parkfield, California, earthquakes of 1966, *Bull. Seism. Soc. Am.* **57,** 1221–1244.

McEvilly, T. V. and L. R. Johnson (1973). Earthquakes of strike-slip type in central California: evidence on the question of dilatancy, *Science* **182,** 581–584.

McEvilly, T. V. and L. R. Johnson (1974). Stability of *P* and *S* velocities from central California quarry blasts, *Bull. Seism. Soc. Am.* **64,** 343–353.

Robinson, R., R. L. Wesson, and W. L. Ellsworth (1974). Variations of *P*-wave velocity before the Bear Valley, California, earthquake of 24 February 1972, *Science* **184,** 1281–1283.

Scholz, C. H., L. R. Sykes, and Y. P. Aggarwal (1973). The physical basis for earthquake prediction, *Science* **181,** 803–810.

Scholz, C. H., M. Wyss, and S. W. Smith (1969). Seismic and aseismic slip on the San Andreas fault, *J. Geophys. Res.* **74,** 2049–2069.

Springer, D. L. and R. L. Kinnaman (1971). Seismic source summary for U.S. underground nuclear explosions, *Bull. Seism. Soc. Am.* **61,** 1073–1098.

Thatcher, W. and T. C. Hanks (1973). Source parameters of southern California earthquakes, *J. Geophys. Res.* **78,** 8547–8576.

Utsu, T. (1973). Temporal variations in travel time residuals of *P* waves from Nevada sources, *J. Phys. Earth* **21,** 475–480.

Whitcomb, J. H., J. D. Garmany, and D. L. Anderson (1973). Earthquake prediction: variation of seismic velocities before the San Fernando earthquake, *Science* **180,** 632–635.

Wyss, M. (1974). Will there be a large earthquake in central California during the next two decades? *Nature* **251** (5471), 126.

Geophysics Department
Stanford University
Stanford, California 94305
(D.M.B., A.G.L., W.W.T.)

Seismographic Station
Department of Geology and Geophysics
University of California
Berkeley, California 94720 (T.V.M.)

Manuscript received December 26, 1974